Conservation Genetics (2025) 26:63–77
https://doi.org/10.1007/s10592-024-01652-4

RESEARCH

Population genomics of a specialized insect, *Tetraopes texanus* (*Coleoptera*: *Cerambycidae*), across a fragmented grassland system

Thomas P. Franzem[1] · Jamie R. Bucholz[2] · Jeffrey D. Lozier[3] · Paige F. B. Ferguson[3]

Received: 16 May 2024 / Accepted: 12 October 2024 / Published online: 25 October 2024

Abstract

Specialist insects are especially susceptible to loss of genetic diversity in the face of habitat destruction and fragmentation. Implementing effective conservation practices for specialist insects will benefit from knowledge of population structure and genetic diversity. Because insects are hyper-diverse, characterizing the population structure of all species within the insect community is untenable, even if focused within a particular habitat type. Thus, concentrating on a single species specialized to a particular habitat type is needed to infer general trends. Here, we investigate the range-wide population genetics of *Tetraopes texanus* Horn 1878 (Coleoptera: Cerambycidae), which provides a useful model of grassland insects due to its' habitat specificity and unique biology. *Tetraopes texanus* occurs primarily in Texas and Oklahoma, into Northern Mexico, and possibly into eastern New Mexico but also occurs in Black Belt prairies of Mississippi and Alabama. Mitochondrial and nuclear DNA (RAD-seq) analysis identified two distinct population clusters of *T. texanus* corresponding to the Texas and Oklahoma population and the Mississippi and Alabama population. Demographic models indicate ongoing, though incomplete, isolation of the two populations, with estimated dates of divergence in the mid-Pleistocene, coinciding with the end of a glacial period and a shift in glacial interval. These results can inform conservation of grassland adapted insects and offers insight to the biogeography of the Gulf Coastal Plain.

Keywords Population genetics · RAD-seq · Insects · Biogeography

Introduction

Nearly all the world's prairies have been converted to human-use or are otherwise degraded (Whiles and Charlton 2006; Gang et al. 2014; Wilsey 2018). Prairie-adapted taxa are likely losing genetic diversity as habitat is fragmented and populations become isolated (Laikre et al. 2010; Freeland 2020). Within prairies, insects are hyper-diverse and as prairies are fragmented and destroyed many insect species are likely impacted, and specialist species are much more likely to lose genetic diversity via genetic drift and inbreeding due to their strict habitat requirements (Bonte et al. 2003; Zayed et al. 2005; Phillipsen et al. 2015; Vidal et al. 2019). Implementing long-term management for prairie insect populations requires more knowledge on the population structure and genetic diversity of natural populations as well as a deeper understanding of historic processes that have shaped modern distributions of insects; this information can be used to identify barriers to gene flow, identify species or populations in need of management, and otherwise inform conservation decisions (Toro and Caballero 2005; Laikre et al. 2010; Freeland 2020). Due to the high diversity of insects, it is not feasible to gain these inferences for all species within the community, even when focusing on insects within a particular habitat type. Thus, identifying general trends by focusing on one or a few species specialized to a particular habitat type is necessary (Phillipsen et al. 2015).

✉ Thomas P. Franzem
tfranzem@kent.edu

Jamie R. Bucholz
bucholzj@vt.edu

Jeffrey D. Lozier
jlozier@ua.edu

Paige F. B. Ferguson
pfferguson@ua.edu

[1] Department of Biological Sciences, Kent State University, Kent, OH, USA

[2] Department of Biological Sciences, Virginia Tech, Blacksburg, VA, USA

[3] Department of Biological Sciences, The University of Alabama, Tuscaloosa, AL, USA

Tetraopes texanus Horn 1878, the Texas Longhorn Milkweed Beetle, is a disjunctly distributed, prairie specialist Longhorn beetle (Coleoptera: Cerambycidae). Due to its' habitat specificity, range, and biology, this species is a useful model in which to elucidate how grassland-specialist insects respond genetically to isolation and habitat fragmentation. *T. texanus* appears to favor prairies and grasslands with calcareous soil of Cretaceous origin. Prairies with this geology are patchily distributed across the gulf coastal plain (Fig. 1) (Peacock and Schauwecker 2003; Echols and Zomlefer 2018). *T. texanus*' range encompasses the prairies of east-central Texas and southern Oklahoma, and the Black Belt Prairies of Mississippi and Alabama (Linsley 1995; Scheifer 1998; Brown 2003; Lingafelter 2007). Populations have also been documented in prairies in Arkansas, Missouri, and into eastern New Mexico and northern Mexico, although they are not as common or widely distributed in these localities (MacRae 1993; Warriner 2004). The geology and distribution of these prairies have resulted in unique biogeographic patterns (Brown 2003; Hill and Barone 2018).

Tetraopes texanus utilizes several milkweed species (*Asclepias*) as a host plant (Linsley 1995; Scheifer 1998). Because of the obligatory association with *Asclepias* spp, *T. texanus* harbors cardiac glycosides in its' body tissues, and thus has few natural predators. Lack of natural predators means their distribution is shaped by habitat area and connectivity, rather than predation pressure (Grainger et al. 2017). *A. viridis* Walter 1788 is the preferred host plant,

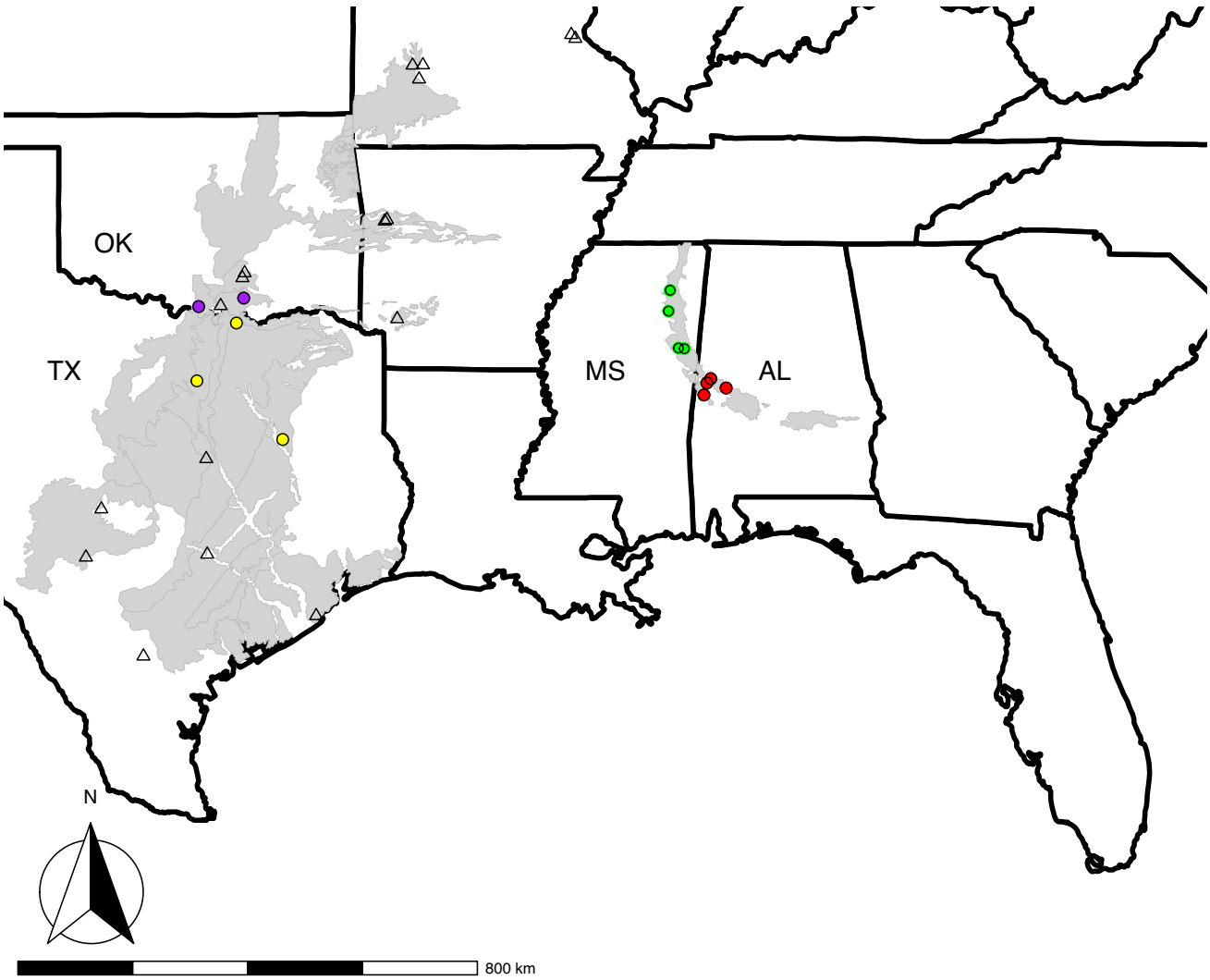

Fig. 1 *Tetraopes texanus* collections sites, color-coded by state. Open triangles are locations where we failed to detect *T. texanus*. Shaded areas are ecoregions that contain suitable habitat for *T. texanus* from the EPA's 'Ecoregion Datatset' (EPA 2024). We note that that these shapefiles may not encompass all *T. texanus* habitat, and that the shapefiles do not imply the entire area within is suitable habitat, but rather likely contains suitable habitat. Additionally, there are no shapefiles that correspond to two locations in eastern Missouri, which are on small, isolated dolomite glades where *T. texanus* has been found in the past

but *T. texanus* can successfully utilize several *Asclepias* species (Linsley 1995; Scheifer 1998; Ali and Agrawal 2017). Adults feed on milkweed leaves and oviposit in the stems of dried grasses and forbs near milkweed stands. After hatching, larvae drop to the soil and feed on milkweed roots (Ali and Agrawal 2017). The ability of *T. texanus* to disperse and locate new suitable habitat patches is not explicitly elucidated in the literature. Previous arguments (Rice 1988) suggest *T. texanus* has limited dispersal and difficulty locating new habitat, given the ecology of the congeneric *T. tetrophthalmus* Forster 1771 (Davis 1984; Lawrence 1988; Rice 1988).

The current disjunct distribution of *T. texanus* is likely a result of Pleistocene climatic shifts isolating populations (Brown 2003; Hill 2015), and putative isolation of the eastern (Mississippi and Alabama) and western (Texas and Oklahoma) populations has likely persisted due to limited dispersal capabilities of the adults. Understanding the population structure and genetic diversity among *T. texanus* populations across its' disjunct distribution and understanding processes from the deep past that shaped its' contemporary distribution may be important for conservation and management of *T. texanus* and can provide insight into how other specialist insects may be impacted under scenarios of increasing habitat fragmentation and isolation (Phillipsen et al. 2015).

Here, we examine the genetic structure of *T. texanus* to elucidate patterns of connectivity, demarcate population structure, and identify climatic and geological processes that may have shaped its' modern distribution. We examined genetic structure and genetic diversity with mitochondrial DNA (mtDNA) sequencing and restriction site-associated DNA (RAD) sequencing. Mitochondrial DNA is widely employed in phylogeographic studies to determine population structure and magnitude of divergence at large spatial scales (Kress et al. 2015; Ghisbain et al. 2020; Bucholz et al. 2022) yet provides limited inference because it is a single genetic marker. RAD-seq provides a large number of genome-wide single-nucleotide polymorphism (SNPs) and has become increasingly common in population and conservation genetics, especially in studies of non-model organisms because it does not require prior genetic information (Andrews et al. 2016; Bucholz et al. 2022). Thus, we employ the two approaches here to retain the benefits of using an established and accepted technique (mtDNA) with the inferential power of the newer RAD-seq approaches; making inference from both approaches can provide a cross-validation of patterns observed (Stobie et al 2019; Bucholz et al 2022). The goal of this study was to identify population clusters of *T. texanus* across its range. Further, we aimed to characterize genetic diversity within populations and test for isolation between eastern and western populations.

Methods

Specimen collection

We collected *Tetraopes texanus* specimens from Alabama and Mississippi in June 2020. In May 2021 we collected *T. texanus* in Mississippi, and in May 2022 we collected specimens from Oklahoma and Texas (Fig. 1; Table S1). We searched for *T. texanus* populations in Arkansas and Missouri in counties where populations have been recorded (Rice 1988; MacRae 1993; Warriner 2004) in May 2022 as well but failed to detect. Sampling sites were identified in Mississippi and Alabama by personal knowledge of *T. texanus* populations on privately owned prairie remnants and suggestions from faculty of the Mississippi Entomological Museum and Mississippi Department of Wildlife, Fisheries, and Parks. Sampling locations in Arkansas, Missouri, Oklahoma, and Texas were located by identifying public lands that contained Blackland prairie, searching for observations of *T. texanus* on iNaturalist, and consulting entomologists at Oklahoma State University, the Enns Entomology Museum, and the Kansas State University Museum of Entomological and Prairie Arthropod Research.

At each sampling site, we identified stands of *T. texanus*' host plants (i.e., *Asclepias viridis* and other *Asclepias* spp.) (Linsley 1995; Scheifer 1998; Warriner 2004) and we searched for beetles during peak daily activity (9 am–5 pm) until we collected ~ 10 individuals. Beetles were collected in a sweep net and each specimen was inspected for identification using the shape and sculpturing of the pronotal callus, the setae on the antennomeres, and the shape of the apical antennomere (Linsley 1995; Lingafelter 2007). Identified beetles were collected in absolute ethanol, stored on ice in the field, and transferred to − 80 °C until dissection.

DNA extraction

We extracted thoracic tissue from each individual and performed DNA extractions using an EZNA Tissue DNA Kit (Omega Bio-tek, Norcross, Georgia). We digested tissue in proteinase K at 55 °C overnight and then followed manufacturer protocols. For the final elution, we eluted into 70 µL for the first elution and 25 µL for the second elution for a final volume of 95 µL. We performed agarose gel electrophoresis with extracted DNA to confirm the presence of genomic DNA of sufficient quality and molecular weight for sequencing and DNA concentrations were measured using an Invitrogen Qubit 2.0 Fluorometer v2.00 (Thermo-Fisher Scientific, Waltham, Massachusetts).

Cytochrome oxidase subunit 1 sequencing

To evaluate divergence among regional populations of *T. texanus* using a well-characterized genetic marker in insects we sequenced the "DNA Barcode" (Hebert et al. 2003; Duennes et al. 2012; Ghisbain et al. 2020) region of the cytochrome oxidase subunit 1 (COI) region of the mitochondrial genome from two individuals per sampling site. The polymerase chain reaction (PCR) to amplify COI used the universal primers LCO1490 and HCO2198 (Folmer et al. 1994) and other reagents following Ghisbain et al. (2020) with the following amplification conditions: initial denaturing at 95 °C for 5 min, followed by 32 cycles of 30 s at 95 °C, 45 s at 53 °C, 45 s at 72 °C, before final elongation of 5 min at 72 °C. PCR products were verified via agarose gel electrophoresis and purified using ExoSap-IT PCR Product Cleanup Reagent (Thermo Fisher Scientific, Waltham, Massachusetts). Products were sequenced in both directions at Eurofins Genomics (Louisville, Kentucky). We automatically assembled reads for each sample into contigs and manually edited sequence data using Geneious Prime v2022.2.2 (https://www.geneious.com).

Restriction site-associated DNA library construction and sequencing

Following extraction, we standardized genomic DNA to ~ 10 ng/µL in 30 µL. We utilized the Best-RAD protocol (Ali et al. 2016) to construct a single nucleotide polymorphism (SNP) dataset, following procedures detailed in Bucholz et al. (2022). In brief, Best-RAD utilizes restriction enzymes to cut DNA into short fragments followed by high-throughput sequencing to produce sequence data for loci adjacent to the restriction enzyme cut sites across the genome (Ali et al. 2016; Andrews et al. 2016). Following standardization, normalized DNA was transferred into two 96-well plates with 68 and 67 samples plus negative controls. DNA was then digested with the restriction enzyme *SbfI*-HF (New England Biolabs, Ipswich, Massachusetts), followed by ligation of oligonucleotide fragments that contained 8 base-pair barcodes. Next, uniquely barcoded samples and negative controls from each plate were pooled and sonicated using a Covaris M220 focused ultrasonicator (COVARIS Inc. Woburn Massachusetts) to generate fragments with a mean size of 550 bp. RAD-tag fragments for each pool were isolated with streptavidin beads and biotinylated groups were removed by *Sbf-1* digestion. We utilized a NEBNext Ultra Kit (New England Biolabs, Ipswich, Massachusetts) to prepare Illumina sequencing libraries with unique dual-index primers for each sample pool with 12 PCR cycles to amplify the RAD-tags. Both pools were sequenced on a single lane of Illumina HiSeqX (Illumina Inc., San Diego, California) by Psomagen Inc (Rockville, Maryland) to produce 150 bp paired end reads.

Bioinformatics and data analysis

Mitochondrial COI sequences

We created a haplotype network based on the number of mutations between different haplotypes using POPART software (Clement et al. 2000; Leigh and Bryant 2015). The number of haplotypes, mean number of pairwise differences, and nucleotide diversity (π) were calculated using Arlequin v3.5.2.2 (Excoffier et al. 2005). We conducted a hierarchical Analysis of Molecular Variance (AMOVA) in Arlequin (Excoffier et al. 1992, 2005) with significance of variance components and *F*-statistics assessed using 1000 permutations to determine if *T. texanus* populations were significantly differentiated within and among regions and among sites within regions.

RADseq data

Illumina reads were demultiplexed and filtered with Stacks v2.62 (Catchen et al. 2013; Rochette et al 2019) using process_radtags (parameters -c, -q, -r, –best-rad, others default). There is no reference genome for *T. texanus*, so we performed de novo locus assembly to identify RADtag loci and alleles with denovo_map.pl, using the parameter –rm-pcr-duplicates set to remove PCR duplicates. The selection of several de novo parameter values for locus assembly can affect results and following the general approach of Paris et al. (2017) we evaluated several values to determine good Stacks parameter settings for the *T. texanus* data set. Following recommendations from Paris et al. (2017), we left the minimum coverage (-m) and allowed mismatches (-N) at the default values, but varied the "distance allowed between stacks" (-M; default M = 2) and the distance allowed between catalog loci (-n; default -n = 1) between one and eight, constraining test parameters such that -n should be equal to M or M ± 1 (Paris et al. 2017). To speed computation during parameter evaluation runs, we ran denovo_map.pl on a subset of the full data comprising 50 individuals (2 regions, 5 populations per region and 5 individuals per population) pooled into a single population. We identified the values that produced the most SNPs in 80% of individuals across populations (the r80 rule from Paris et al. 2017). Ultimately, we selected denovo_map.pl setting -M = 2 and -n = 2 as the best parameter settings for the full data set (other parameters default).

We next used the populations function in Stacks to filter data, calculate diversity statistics, and export data in variant call format (vcf). We used a population map that retained

114 samples from the 13 population with < 50% missing data in preliminary analyses. For most analyses presented, we used a data set filtered to retain all sequenced sites (variant or invariant) sequenced in 70% of samples (R70), or a thinned data set that included a random SNP per RAD-tag locus in 70% of samples to minimize linkage effects (R70 + write-random-snp). Because non-neutral SNPs can potentially impact estimates of parameters used to estimate population history and demography, to remove effects of potentially non-neutral sites we used Bayescan 2.1 (Foll and Gaggiotti 2008; Fischer et al. 2012), which aims to detect candidate loci under selection from allele frequency differences among population using Bayes factors. We ran the program with default settings using the full SNP set (unthinned) and identified candidate SNPs at a false discovery rate corrected significance of $q \leq 0.05$. Stacks catalog loci containing any candidate SNPs were then provided as a blacklist for removal in final populations runs as above (full and thinned R70). Note, given the small size of this RAD-tag data set and lack of a reference genome, we are not focused on identifying the possible adaptive role of candidate SNPs, but rather on identifying loci that may behave non-neutrally and might bias estimates of population structure and diversity without invoking a causal mechanism. Removing putative candidate loci had only marginal qualitative effects on results (results for full data presented in Table S3).

We used Stacks to calculate diversity statistics. The thinned R70 data set was used to determine the number of private alleles, expected heterozygosity (H_E), observed heterozygosity (H_O), and the inbreeding coefficient (F_{IS}); the dataset including all sequenced variant and invariant sites was used to calculate nucleotide diversity (π).

Unless otherwise stated, all remaining analyses were conducted in R v4.0.3 (R Core Team, 2018). We used the R package *vcfR* v1.14.0 (Knaus and Grunwald 2017) to import data and convert to a genind object. Pairwise measures of genetic differentiation (F_{ST}) were computed in the R package *hierfstat* (Goudet and Jombart 2022) via the function *genet.dist* with method "WC84" (Weir and Cockerham 1984). We determined pairwise geographic distances between sites via the Geographic Distance Matrix Generator from the American Museum of Natural History (Ersts 2023) using the 'WGS84' reference system. We used pairwise geographic distances and F_{ST} values to evaluate isolation-by-distance using Mantel tests (Smouse et al. 1986) with the function *mantel* in the R package *vegan* v2.6.4 (Oksanen et al. 2022). We compared F_{ST} and geographic distance for the full dataset and for subsets of the dataset corresponding to the western and eastern populations identified in analyses above (see Results).

We assessed genetic structure using a principal component analysis (PCA) by first using the *tab* function to replace missing data with mean allele frequency (Jombart and Ahmed 2011), and then using the *dudi.pca* function in the R package *ade4* v1.7.22 (Dray and Dufour 2007). We conducted a PCA on the full dataset and on subsets of the dataset corresponding to the western and eastern populations and retained two axes (Fig. S3). We assessed individual genetic clustering into populations with sNMF (Frichot and François 2015) using the *snmf* function in the R package *LEA* v3.2.0 (Frichot and François 2015) with K (number of genetic populations) determined by the value producing the lowest cross-entropy (Frichot and François 2015). We assessed populations for $K = 1$ to 10 with 100 repetitions.

We conducted a hierarchical analysis of molecular variance (AMOVA) to estimate SNP partitioning within and among sampling locations to determine whether populations were significantly differentiated within regions and among sites (Excoffier et al. 1992). We utilized Arlequin (Excoffier et al. 2005) with significance of variance components and F-statistics assessed using 1000 permutations.

Demographic analyses

Results above indicated two major population clusters (eastern and western; see Results), so to assess divergence timing, population size changes, and migration patterns, we performed demographic analyses using a two-population isolation with migration model in GADMA 2.0.0 (Noskova and Borovitskiy 2023). GADMA is a method for demographic inference from site frequency spectrum (SFS) data that uses a genetic algorithm approach to perform unsupervised parameter estimation and model selection under a given model.

We generated a folded two-dimensional SFS for analysis from the thinned R70 data set using easySFS (https://github.com/isaacovercast/easySFS) and downprojected the SFS to retain 46 haploid chromosomes per population in δaδi sfs format (Gutenkunst et al. 2009) for use in GADMA. For conversion to real world values for time (T in years, assuming one generation per year for the univoltine *T. texanus*) and population size (N_e, effective individuals), we determined effective genome length (L) of our data following the GADMA manual instructions with the equation [(1,183/20,785) * 1,101,838] = 67,712 effective bp. Values are characteristics of the data set, which had a sequenced genome size of 1,101,838 bp with 20,785 SNPs, which we thinned to retain a final set of 1,467 independent SNPs, of which 1,183 were retained in the downprojected SFS. Conversion also requires an estimate of the mutation rate (μ). No μ estimates are available, so following other genome-scale studies of beetles, including Cerambycidae (Cui et al. 2022; Araki and Sota 2023; De Vivo et al. 2023), we applied a rate of 2.9×10^{-9} per site per generation from *Heliconius melpone* (Keightley et al.

2015). Although this rate will not be exact, this value falls within the range reported for many other insects (e.g., *Chironomus* = 2.1×10^{-9}, *Bombus* = 3.6×10^{-9}, *Drosophila* = 2.8–3.5×10^{-9}) (Keightly et al. 2014; Liu et al. 2017; Oppold and Pfenninger 2017). For model inference we employed the MOMENTS (Jouganous et al. 2017) engine within GADMA and specified a demographic model for unlinked SNPs (parameter setting Linked: False) where an ancestral population divided into the two contemporary populations (parameter setting Initial Structure: 1,1), that were each allowed to undergo a linear or exponential size change and experience asymmetrical migration, followed by a Final Structure that allowed for a second post-divergence phase for population size and migration (Final Structure: 2,2). We report the best models using AIC from 20 simultaneous replicate runs. We estimated 95% confidence intervals for parameters under the AIC-selected MOMENTS model using the gadma-run_ls_on_boot_data and gadma-get_confidence_intervals scripts on 200 bootstrapped SFS replicates as specified in the GADMA manual (gadma.readthedocs.io). To generate bootstraps, we resampled the thinned vcf file 200 times with replacement and generated the SFS for each pseudoreplicate using easySFS as above.

Results

COI dataset

To obtain an initial view of phylogeographic divergence across the range of *T. texanus*, we analyzed a 673 bp fragment of the COI mtDNA gene from 24 individuals from 13 locations (NCBI GENBANK identifiers: OR613385-OR613408). We identified 17 haplotypes that were divided into eastern and western regions, with 9 haplotypes belonging to the eastern region, and 8 belonging to the western region, and 4 mutations separating the ancestral haplotypes of the populations (~0.59% divergence; Fig. 2). Assuming the commonly used insect mitochondrial pairwise mutation rate of ~2.3435% divergence per million years (Brower 1994), this would correspond to a date of sequence divergence of approximately 251,000 years before present (ybp). Mean nucleotide diversity among both regions was similar (Table 1). AMOVA showed significant genetic differentiation among the regional clusters ($F_{CT} = 0.621$, $p < 0.0001$) as well as among sites overall ($F_{ST} = 0.674$, $p < 0.0001$) but not among sites within clusters ($F_{SC} = 0.140$, $p = 0.0997$) (Table 2).

SNP dataset

Illumina sequencing of the BestRAD libraries yielded an average of 4,943,842 (sd = 5,142,084) retained reads per sample after demultiplexing (NCBI SRA Identifiers: SAMN39530086–SAMN39530199). Using filtering criteria that removed catalog loci with > 30% missing data and with SNPs putatively identified as non-neutral by Bayescan, the final data set included 114 individuals from 13 collection locations with 1,101,838 bp of total sequence (mean depth of 39.4x) and 20,785 variable sites. Thinning the data set to one SNP per locus retained 1,467 SNPs, with nearly all SNPs genotyped in every population (Table 3).

The SNP dataset suggested that *T. texanus* from western populations harbored greater genetic diversity than those from eastern populations across all metrics of diversity. Eastern populations had strongly reduced H_O, H_E, π, and numbers of private alleles compared to western populations (Table 3). H_O was similar to, but slightly lower than H_E across most populations, which produced slightly positive estimates of F_{IS} (Table 3). Using alternative thresholds for missing data or retaining Bayescan outliers in the data set produced similar diversity patterns as presented in Table 3, indicating results are robust to the SNP filtering criteria (Table S4).

Pairwise F_{ST} among collection sites ranged from 0.003 to 0.211 (Table S2), with low values within each region and higher values found between the regions. Mantel tests of F_{ST} and pairwise geographic distance showed strong isolation between the eastern and western regions (Fig. 3a Mantel $r = 0.8738$, $p = 0.001$). Further, we detected Isolation-By-Distance within eastern populations (Fig. 3c Mantel $r = 0.6113$, $p = 0.003$), but not within western populations, with the Mantel test failing to reject the null hypothesis (Fig. 3b Mantel = -0.2604, $p = 0.683$).

As for the COI dataset, the PCA and sNMF analyses of SNPs identified genetic clusters corresponding to the western and eastern regions (Fig. 4; Fig. 5). The sNMF analysis identified $K = 2$ as the optimal number of ancestral populations based on lowest cross-entropy (Fig. 5; Fig. S1; Fig. S2). The two populations indicated by sNMF comprised all the individuals from the western region, and all the individuals from the eastern region, respectively, although the admixture coefficients indicated some degree of imperfect assignment for most individuals (Fig. 5). Both the PCA and sNMF analyses produced similar results with more stringent missing data filtering despite reduced SNP numbers (Fig. S4; Fig. S5). AMOVA showed significant genetic differentiation among two regional clusters ($F_{CT} = 0.111$, $p < 0.0001$) as well as among sites within clusters ($F_{SC} = 0.055$, $p < 0.0001$) and among sites overall ($F_{ST} = 0.159$, $p < 0.0001$) (Table 4).

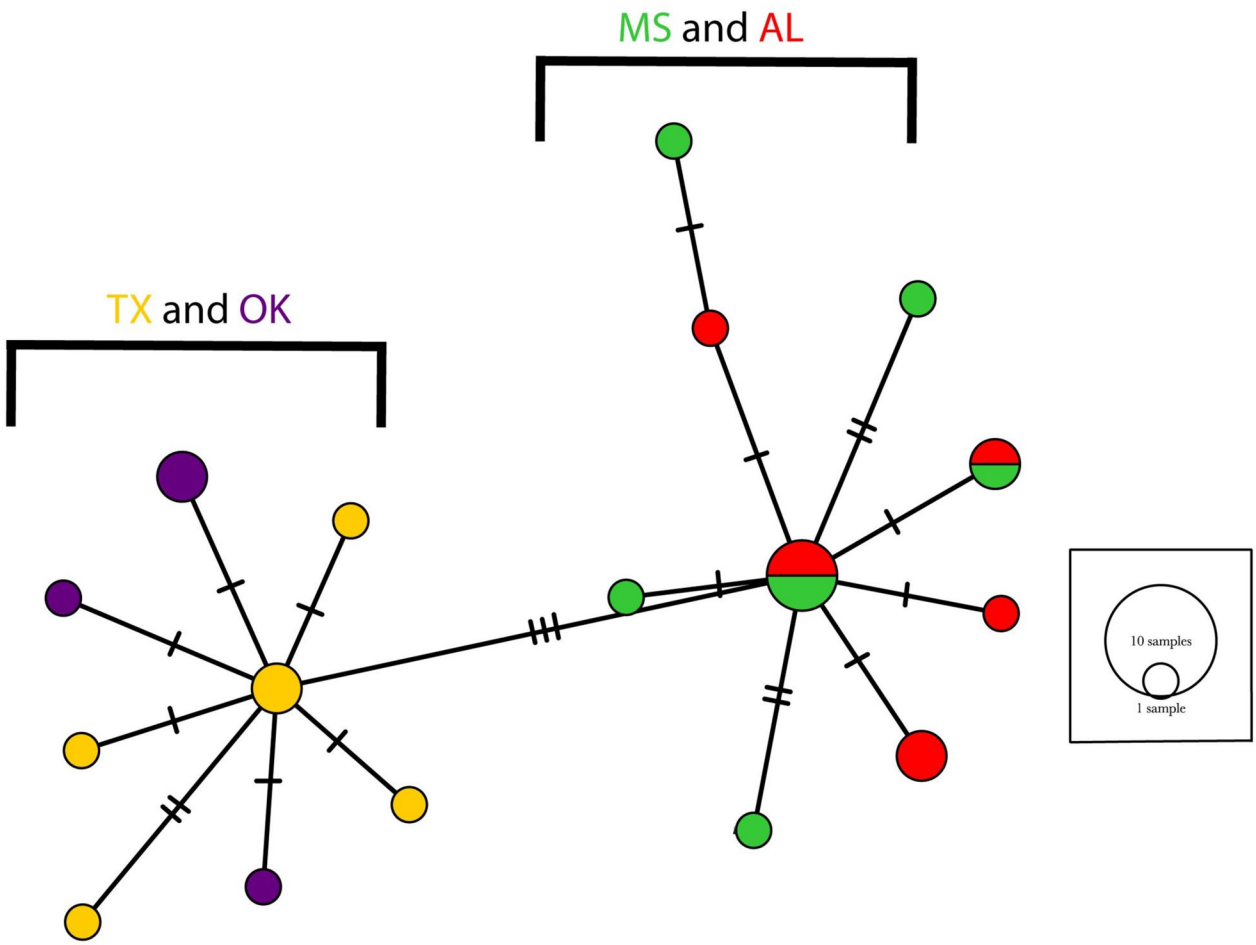

Fig. 2 Mitochondrial COI haplotype network of 24 *Tetraopes texanus* specimens from 13 collection locations across Mississippi (MS), Alabama (AL), Texas (TX), and Oklahoma (OK). Hash marks in connecting lines indicate number of substitutions separating haplotypes

Table 1 Number of *Tetraopes texanus* individuals sequenced for mitochondrial COI from the west (Texas and Oklahoma) and east (Mississippi and Alabama), the mean number of pairwise differences among haplotypes, and mean nucleotide diversity (π)

Region	N sequenced	Mean No. of pairwise differences	π
West	10	1.755556	0.002609
East	14	1.791209	0.002662

The best demographic model for GADMA selected by AIC was a simple isolation with migration model (Fig. 6). Divergence of eastern and western populations was inferred to have occurred in the mid-Pleistocene (T_{Div} = 203,843 ybp, 147,196 – 290,767 95% CI) from a relatively small ancestral population to create a post-divergence eastern population comparable in size to the ancestral population and a much

Table 2 Analysis of molecular variance (AMOVA) for *Tetraopes texanus* using mitochondrial COI sequence data

Source of variation	Sum of squares	Percentage variation	F-statistics	p
Among Groups	18.207	62.106%	F_{CT}: 0.621	< 0.0001***
Among Populations Within Groups	11.043	5.321%	F_{SC}: 0.140	0.0997
Within Populations	8.500	32.572%	F_{ST}: 0.674	< 0.0001***
Total	37.750			

Table 3 Diversity statistics for *Tetraopes texanus* (<30% missing data), including population (state and locality abbreviation; see Fig. 1), sample size (N), number of sequenced variant + invariant sites (Total sequenced bp), total number of variant sites (Variant bp), number of SNPs thinned to 1 per locus, percent SNPs polymorphic within each population (% variable SNPs), number of private alleles, observed heterozygosity (H_O), expected heterozygosity (H_E), F_{IS}, and nucleotide diversity (π), with standard errors in parentheses. Diversity statistics are calculated using 1 SNP per locus except π, which is calculated across all sequenced sites

Population	Region	N	Total sequenced bp	Variant bp	SNPs (1 per locus)	% variable SNPs	Private alleles	H_O	H_E	F_{IS}	π
AL_LOV	East	12	1,101,838	20,785	1467	0.03	35	0.058 (0.004)	0.062 (0.003)	0.022 (0.040)	0.0014 (0.0000)
AL_MOU	East	5	1,101,838	20,785	1467	0.02	11	0.052 (0.004)	0.053 (0.003)	0.018 (0.023)	0.0013 (0.0000)
AL_SHR	East	9	1,101,838	20,785	1467	0.03	19	0.051 (0.003)	0.057 (0.003)	0.025 (0.035)	0.0014 (0.0000)
AL_UWA	East	11	1,101,838	20,785	1467	0.03	16	0.052 (0.003)	0.057 (0.003)	0.024 (0.037)	0.0013 (0.0000)
MS_BOL	East	10	1,101,838	20,785	1467	0.03	21	0.055 (0.003)	0.060 (0.003)	0.026 (0.038)	0.0014 (0.0000)
MS_BPR	East	10	1,101,838	20,785	1467	0.03	15	0.051 (0.003)	0.059 (0.003)	0.030 (0.041)	0.0013 (0.0000)
MS_CHP	East	10	1,101,838	20,785	1467	0.02	20	0.047 (0.003)	0.052 (0.003)	0.023 (0.037)	0.0012 (0.0000)
MS_CHS	East	8	1,101,838	20,785	1467	0.03	17	0.052 (0.004)	0.057 (0.003)	0.021 (0.030)	0.0013 (0.0000)
OK_CRT	West	8	1,101,838	20,785	1467	0.04	127	0.075 (0.004)	0.085 (0.004)	0.044 (0.036)	0.0019 (0.0000)
OK_TIS	West	9	1,101,838	20,785	1467	0.04	140	0.088 (0.004)	0.089 (0.004)	0.025 (0.037)	0.0019 (0.0000)
TX_FWN	West	8	1,101,050	20,778	1466	0.05	162	0.083 (0.004)	0.089 (0.004)	0.038 (0.035)	0.0019 (0.0000)
TX_GEN	West	8	1,101,837	20,784	1467	0.04	94	0.067 (0.004)	0.077 (0.004)	0.045 (0.037)	0.0017 (0.0000)
TX_HAM	West	6	1,099,906	20,765	1462	0.03	87	0.071 (0.004)	0.074 (0.004)	0.028 (0.030)	0.0018 (0.0000)

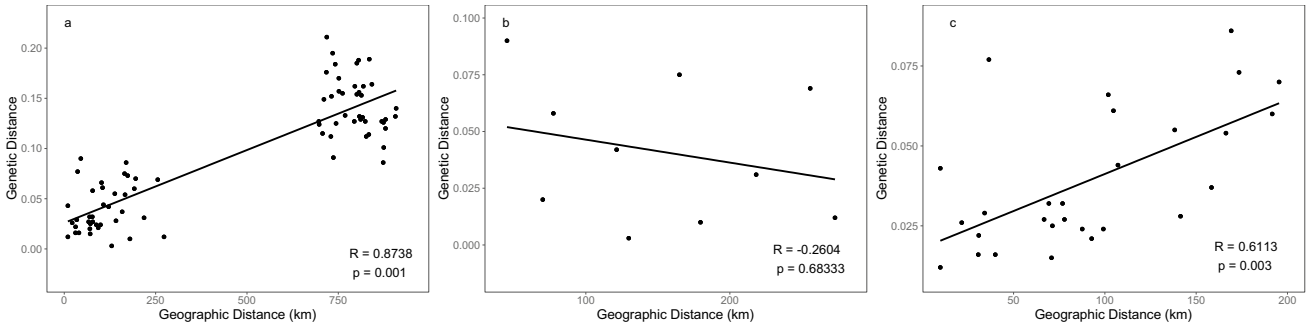

Fig. 3 Mantel test for pairwise landscape distances between sampling sites and estimates of F_{ST} RAD-seq SNP data for **a** the entire sampling extent, **b** the Texas and Oklahoma populations, **c** the Mississippi and Alabama populations

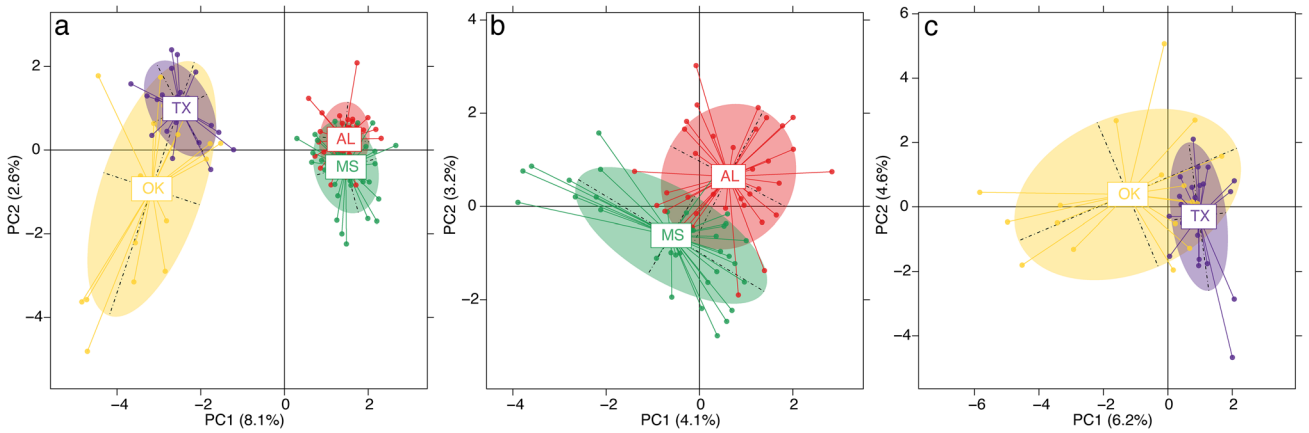

Fig. 4 Principal component analysis of *Tetraopes texanus* populations for **a** the entire sampling extent, **b** the Texas and Oklahoma populations, and **c** the Mississippi and Alabama populations. Axes labels indicate the percentage of variation described by the respective principal component

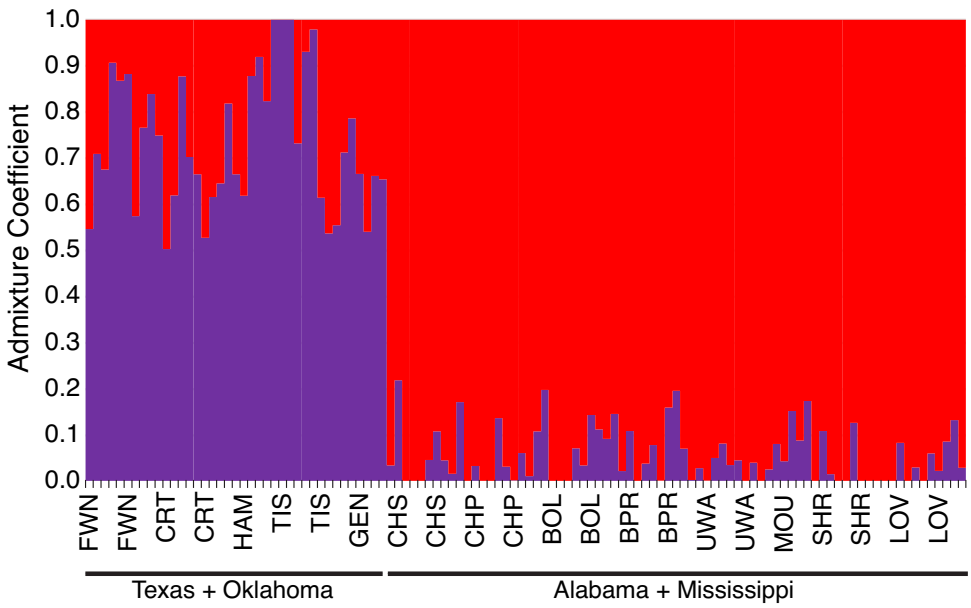

Fig. 5 Results from SNMF admixture analysis for $K = 2$. The primarily red cluster corresponds to the Mississippi and Alabama populations, and the primarily purple cluster corresponds to the Texas and Oklahoma populations

Table 4 Analysis of molecular variance (AMOVA) for *Tetraopes texanus* using RAD-seq SNP data

Source of Variation	Sum of Squares	Percentage Variation	F-Statistics	p
Among Groups	617.613	11.05846%	F_{CT}: 0.111	<0.0001***
Among Populations Within Groups	1014.571	4.88%	F_{SC}: 0.055	<0.0001***
Within Populations	8525.084	84.07%	F_{ST}: 0.159	<0.0001***
Total	10,157.286			

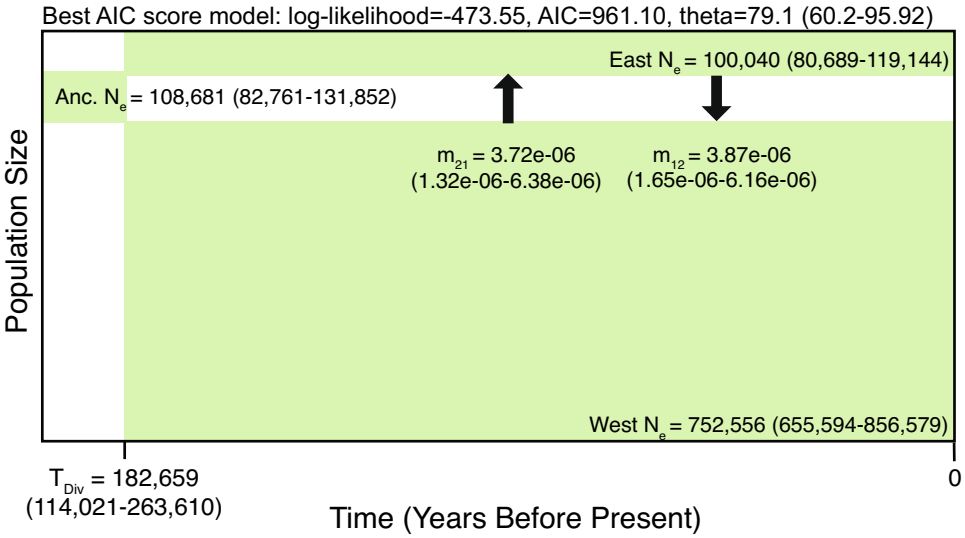

Fig. 6 Best fitting GADMA2 demographic model. Times (in years before present), effective population sizes (N_e, in individuals) migration rates (m, in proportion of migrants in population per generation) are presented in physical units using a mutation rate $\mu = 2.9 \times 10^{-9}$ per site per generation

larger western population, with ongoing low but significant bidirectional gene flow (Fig. 6).

Discussion

We identified two genetically distinct populations of *T. texanus* in both SNP and COI data. Mitochondrial COI sequences and RADseq data analyses support two populations of *T. texanus* corresponding to the western part of its range and the eastern part of its range. Both data sets suggest mid-Pleistocene divergence between the two regions, with the western region exhibiting larger population sizes and greater genetic diversity than in the east.

A recent phylogenomic study on *Tetraopes* found that the genus originated in Central America and expanded and diversified in the late-Miocene and early-Pleistocene (Gutierrez-Trejo et al. 2024). Our results provide a complement to this genus-level investigation and suggest *T. texanus* expanded into present-day Texas via Mexico in the late-Miocene, experienced a population and range expansion through the early-Pleistocene, followed by separation of the eastern and western populations in the mid-Pleistocene. The strong population structure we observed provides evidence of substantial, although incomplete, ongoing isolation of the eastern and western populations as a function of spatial separation between regions, supporting previous arguments (Rice 1988) that *T. texanus* should have limited dispersal (Davis 1984; Lawrence 1988; Rice 1988). Such limited dispersal is expected for the degree of habitat specialization and host plant specificity exhibited by *T. texanus,* as the more specialized an organism is, the lower the propensity for dispersal (Bonte et al. 2003). The habitat that *T. texanus* requires is fragmented and isolated in a matrix of unsuitable habitat, thus attempts at long-distance dispersal carry high risk (Phillipsen et al. 2015). Genetic data suggest dispersal is possible within each geographic region, but that the eastern and western regional clusters are separated by broad areas of unsuitable habitat (Fig. 1) that limits the potential for extensive gene flow, as indicated by the low dispersal rates estimated by GADMA and lack of overlapping mtDNA haplotypes between the regions.

The disjunct distribution of *T. texanus* reflects the biogeographic history of southeastern prairies (Brown 2003; Hill 2015). However, the nature of disjunct insect distributions has not been well-characterized in the region (Hill and Barone 2018). The leading hypothesis concerning the origin of disjunct insect distributions across the gulf-coastal plain is that suitable habitat once connected southeastern prairies to western prairies during the Pleistocene (Brown 2003; Noss 2013). Hill (2015) investigated the genetics of southeastern grasshoppers, some

of which display a disjunct distribution with populations in western prairies, like *T. texanus*. They concluded the distribution of grasshoppers was likely the result of a late Miocene and early Pleistocene vicariance event that isolated populations when prairie habitat was converted to woodlands and the Mississippi river opened following climate shifts. The genetic patterns exhibited by eastern populations of *T. texanus* are consistent with a historical founder-effect as the Black Belt prairies were colonized by migrants from the western part of the range, although the largely symmetrical gene flow inferred by GADMA makes it difficult to directly test this hypothesis with the current data. The larger effective population size in the western population may simply be a result of the much more extensive habitat area available compared to the narrower Black Belt prairie in Alabama and Mississippi (Fig. 1), and even before contemporary fragmentation and habitat destruction is considered, the western region would likely have supported a larger population. Both the western and eastern parts of the range have experienced severe fragmentation and degradation, and purportedly less than 1% of intact native prairies remain (Hill and Barone 2018; Augustine et al. 2021), but the availability of more standing genetic variation in the western range may be reducing the deleterious genetic effects of contemporary fragmentation relative to the eastern populations.

The consistent divergence time estimates from both COI and RADseq data suggest the disjunct distribution of *T. texanus* has origins in the mid-Pleistocene, corresponding to the end of a mid-Pleistocene glaciation and a shift in glacial intervals from 40,000 years to 100,000 years (Delmas et al. 2011). However, climatic shifts do not fully explain the current distribution of *T. texanus*, since there were likely subsequent glacial periods where prairie habitat may have been extensive across the gulf-coastal plain, allowing for rejoining of the eastern and western populations (Delmas et al. 2011). The distribution of *T. texanus'* host plants in conjunction with the distribution of calcareous soils may explain the unique distribution of *T. texanus* and the persistent isolation of the western and eastern populations, although this is speculative. The distribution of *T. texanus* and its primary host plant (*A. viridis*) largely tracks the southern distribution of the Western Interior Seaway (WIS), a shallow sea that covered a significant portion of North America during the Cretaceous period (Wright 1987). *T. texanus* is associated with calcareous soils and limestone prairies, which are distinctive geological features associated with the WIS; the Blackland prairies of Texas and Oklahoma and the Black Belt prairie of Mississippi and Alabama occur on rock formations derived from the WIS (Peacock and Schauwecker 2003).

It is possible calcareous grasslands were once more extensive between the Blackland prairies of Texas and Oklahoma and the Black Belt of Mississippi and Alabama. Indeed, today there are small calcareous prairies in Louisiana, southern Arkansas, and western Mississippi (Peacock and Schauwecker 2003), which suggest limestone formations that gave rise to Blackland prairies may have once been more extensive. However, the flow of water through the Mississippi embayment may have eroded these limestone formations or covered them in significant alluvial deposits over time, creating the current spotty distribution of small calcareous prairies in Louisiana (Cushing et al. 1964; MacRoberts et al. 2003). We hypothesize the initial movement of *T. texanus* from west to east was achieved via dispersal across calcareous prairie patches spanning northern Louisiana and southern Arkansas, which may have been more extensive in the Pleistocene. During drier glacial periods, where open habitat would have been more common across the gulf coastal plain, *T. texanus* would have been able to move between limestone prairie stepping-stones. During wetter interglacial periods, woodlands would be more common, but open habitat would have persisted on limestone formations because the high shrink-swell potential of the soil, underlying geology, and natural pyro-dynamics can act to prevent transition to woodlands (Brown 2003; Schotz and Barbour 2009). Thus, *T. texanus* populations may have become isolated on islands of limestone prairies during interglacial periods. The estimated divergence times approximately coincide with the end of a mid-Pleistocene glaciation, and the beginning of an interglacial period that would have lasted approximately 100,000 years (Kawamura et al. 2007). If there were populations of *T. texanus* on the smaller limestone prairies of Louisiana, this period of isolation may have driven these geographically intermediate populations extinct.

An interesting avenue of future research would be to investigate other Cerambycids that purportedly display a disjunct distribution like *T. texanus*. Multispecies comparative phylogeography is a powerful tool for evolutionary inference (Edwards et al. 2022) and may be especially useful to corroborate hypotheses concerning the origin of the unique biogeographic patterns present across the gulf coastal plain (Hill 2015; Hill and Barone 2018). For example, *Ataxia brunnea* Champlain and Kull 1926 and *Dylobolus rotundicollis* Thomson 1868 display similar patterns of disjunction as *T. texanus* (Scheifer 1998; Brown 2003). It would be informative to see if the date of divergence among these Cerambycids is similar, or if the apparent extended divergence time of *T. texanus* is unique due to the distribution of its' host plants, apparent affinity for calcareous soils, and limited dispersal capabilities. Information on contemporary genetic structure of these beetle species, especially relating to patterns of co-divergence and co-migration (Xue and Hickerson 2020), would provide greater context to the results presented here.

Another interesting avenue of research would be to investigate the degree to which *T. texanus*' range is driven by the distribution of its' host plants, the distribution of calcareous soils, and the host specificity it displays. Intuitively, it makes sense that *T. texanus* would track the distribution of the plants it feeds on in all life-stages, however the reported utilization of several different host plants that occur both on and off calcareous soils confound this explanation some (Ali and Agrawal 2017). For example, in Mississippi and Alabama, the distribution of *A. viridis* is concentrated on the calcareous soils of the Black Belt prairies, but does occur elsewhere in the state, along with other suitable *Asclepias* spp (USDA NRCS Plant Data Team 2024). Yet *T. texanus* is restricted to the Black Belt prairies. It could be that suitable hosts only occur in high enough densities in the Black Belt, or, as discussed above, *T. texanus* may prefer calcareous soils for larval development. Future research disentangling the influence of edaphic conditions and host specificity on *T. texanus'* distribution can further contextualize the patterns described here, provide insight into the biology and ecology of *T. texanus*, and inform conservation efforts.

One challenge to complete inference about the mechanism driving observed genetic structure is we were unable to obtain samples from existing intermediate populations (e.g., Arkansas and Missouri) despite surveys where *T. texanus* has been recorded (MacRae 1993; Warriner 2004). The large divergence estimates from the RAD-seq and COI data (e.g., mutational separation of haplotypes and absence of shared sequences among regions) suggest substantial regional divergence, but characterizing the genetics of these relict populations would provide greater context to contemporary population structure and assist in understanding past and present patterns of gene-flow and barriers to dispersal. A priority of future research should be to sample individuals from Arkansas and Missouri and understand where these populations fit into the population structure identified here.

The results of this work have implications for conservation of *T. texanus*. Indeed, *T. texanus* is listed as a species of greatest conservation need in the state of Arkansas (Arkansas Game and Fish Commission, 2016). Despite high abundance where populations are established, current populations are discontinuous and the specific habitat requirements and limited dispersal ability make *T. texanus* susceptible to the deleterious effects of habitat loss (Bonte et al. 2003; Phillipsen et al. 2015). Our results suggest that regional populations are likely to require specific management as ongoing gene flow is rare, and demographic analysis indicate the eastern populations have reduced effective population size that may make these populations particularly vulnerable. As more suitable habitat is destroyed and populations become increasingly isolated, loss of genetic diversity as a function of genetic drift and inbreeding will become more pronounced (Freeland 2020). The results presented here offer insight into how other specialist insects may respond to increasing fragmentation. *T. texanus* will not necessarily reflect how all grassland insects respond to fragmentation but can serve as a useful proxy for specialist insects, which may lose genetic diversity under scenarios of increasing isolation and reduced habitat area (Bonte et al. 2003; Phillipsen et al. 2015). Conservation of specialist insects begins with conservation of the habitat they depend on.

Supplementary Information The online version contains supplementary material available at https://doi.org/10.1007/s10592-024-01652-4.

Acknowledgements Thank you to the state, federal, and tribal organizations that helped locate sampling sites, secure collection permits, and coordinate field logistics. Thank you to the private landowners that allowed us to collect beetles on their property and for their prairie conservation efforts. Thank you to personnel at Hagerman NWR, Brazoria NWR, and Tishomingo NWR (particularly Megan Gallagher and Justin Roach). Claude Jenkins, JoVonn Hill, and John Gruchy helped locate sampling sites in Alabama and Mississippi. Kevin Shaw helped with field work in 2021. Special thanks to Cassie Bell for her assistance in the 2022 field season. Thank you to Sam Heraghty and Kelton Verble for their assistance with lab work and data analysis.

Author Contributions Thomas Franzem, Paige Ferguson, and Jeffrey Lozier all contributed to study conception and design and co-authored the grant proposal that primarily funded this work. Thomas Franzem planned and conducted all field work and obtained relevant national, state, and property-level collection permits. Paige Ferguson provided materials and logistical support for field work. Jeffrey Lozier provided lab space, lab equipment, guidance for lab work, and guidance for bioinformatics. Thomas Franzem performed DNA extraction for all the specimens and standardized DNA samples. Jamie Bucholz prepared DNA libraries, provided feedback and training on lab work, assisted in data analysis, and provided example code for some of the analyses presented here. Thomas Franzem conducted the data analysis with the input of Jamie Bucholz and Jeffrey Lozier. Jeffrey Lozier conducted the demographic analysis and created Fig. 6. Thomas Franzem prepared the manuscript, and Jeffrey Lozier provided comments and wrote the methods section for the Demographic Analysis. All authors read and approved the manuscript prior to submission.

Funding This work was supported by the College Academy of Research Scholarship and Creative Activity grant from the University of Alabama College of Arts and Sciences, the Arts and Sciences Support for Undergraduate Research from the University of Alabama College of Arts and Sciences, and Research Travel Awards from the University of Alabama Graduate School. Jeffrey Lozier and Jamie Bucholz were supported by National Science Foundation grants (DEB-1831512 and EF-1921585) during work on this project. Any opinions, findings, and conclusions or recommendations expressed in this material are those of the authors and do not necessarily reflect the views of the National Science Foundation.

Data availability The SNP and mtDNA datasets generated and analyzed here are available in the National Center for Biotechnology Information's Sequence Read Archive and Genbank, respectively (NCBI SRA Identifiers: SAMN39530086 – SAMN39530199; NCBI GENBANK identifiers: OR613385-OR613408). Further, we have created a figshare project for this study that contains the code used for analysis

and figure generation (project title: Population Genetics of *Tetraopes texanus* (Coleoptera: Cerambycidae)).

Declarations

Competing Interests The authors have no relevant financial or non-financial interests to disclose.

References

Ali JG, Agrawal AA (2017) Trade-offs and tritrophic consequences of host shifts in specialized root herbivores. Funct Ecol 31:153–160

Ali OA, O'Rourke SM, Amish SJ, Meek MH, Luikart G, Jeffres C, Miller MR (2016) RAD capture (Rapture): flexible and efficient sequence-based genotyping. Genetics 202:389

Andrews KR, Good JM, Miller MR, Luikart G, Hohenlohe PA (2016) Harnessing the power of RADseq for ecological and evolutionary genomics. Nat Rev Genet 17:81–92

Araki Y, Sota T (2023) Whole-genome resequencing reveals recent divergence of geographic populations of the dung beetle *Phelotrupes auratus* with color variation. Ecol Evolut. https://doi.org/10.1002/ece3.9765

Arkansas Game and Fish Commission, 2016, agfc.com, "Scientific Collection Permits", accessed 28 Sep 2023 https://www.agfc.com/en/wildlife-management/scientific-collection-permits/

Augustine D, Davidson A, Dickinson K, Van Pelt B (2021) Thinking like a grassland: challenges and opportunities for biodiversity conservation in the great plains of north America. Rangel Ecol Manage 78:281–295

Bonte D, Vandenbroecke N, Lens L, Maelfait JP (2003) Low propensity for aerial dispersal in specialist spiders from fragmented landscapes. Proc Royal Soc B-Biol Sci 270:1601–1607

Brower AVZ (1994) Rapid morphological radiation and convergence among races of the butterfly *Heliconius erato* inferred from patterns of mitochondrial DNA evolution. Proc Natl Acad Sci USA 91:6491–6495

Brown RL (2003) Paleoenvironment and biogeography of the mississippi black belt: evidence from insects. In: Peacock E, Schauwecker T (eds) Blackland prairies of the Gulf Coastal Plain, 1st edn. The University of Alabama Press, Tuscaloosa, AL, pp 11–26

Bucholz JR, Sard NM, VanTassel NM, Lozier JD, Morris TJ, Paquet A, Zanatta DT (2022) RAD-tag and mitochondrial DNA sequencing reveal the genetic structure of a widespread and regionally imperiled freshwater mussel, *Obovaria olivaria* (*Bivalvia*: *Unionidae*). Ecol Evol. https://doi.org/10.1002/ece3.8560

Catchen J, Hohenlohe PA, Bassham S, Amores A, Cresko WA (2013) Stacks: an analysis tool set for population genomics. Mol Ecol 22:3124–3140

Clement M, Posada D, Crandall KA (2000) TCS: a computer program to estimate gene genealogies. Mol Ecol 9:1657–1659

Cui MM, Wu YK, Javal M, Giguère I, Roux G, Andres JA, Keena M, Shi J, Wang BD, Braswell E, Pfister SE, Hamelin R, Roe A, Porth I (2022) Genome-scale phylogeography resolves the native population structure of the Asian longhorned beetle, *Anoplophora glabripennis* (Motschulsky). Evol Appl 15:934–953

Cushing EM, Boswell EH, Hosman RL (1964) General geology of the mississippi embayment. U.S. department of the interior. geological survey professional paper. 448-B.

Davis MA (1984) The flight and migration ecology of the red milkweed beetle (*Tetraopes tetraophthalmus*). Ecology 65:230–234

Delmas M, Calvet M, Gunnell Y, Braucher R, Bourles D (2011) Palaeogeography and Be-10 exposure-age chronology of middle and late pleistocene glacier systems in the northern pyrenees: implications for reconstructing regional palaeoclimates. Palaeogeogr Palaeoclimatol Palaeoecol 305:109–122

De Vivo M, Chou MH, Wu SP, Kuan YH, Chen WY, Wang LJ, Morgan B, Phang GJ, Huang JP (2023) Genomic tools for comparative conservation genetics among three recently diverged stag beetles (*Lucanus*, Lucanidae). Insect Conservation and Diversity 16:853–869

Dray S, Dufour AB (2007) The ade4 package: Implementing the duality diagram for ecologists. J Stat Softw 22:1–20

Duennes MA, Lozier JD, Hines HM, Cameron SA (2012) Geographical patterns of genetic divergence in the widespread mesoamerican bumble bee Bombus ephippiatus (*Hymenoptera*: *Apidae*). Mol Phylogenet Evol 64:219–231

Echols SL, Zomlefer WB (2018) A synopsis of southeastern blackland prairies. In: Hill JG, Barone JA (eds) Southeastern grasslands: biodiversity, ecology, and management, 1st edn. The University of Alabama Press, Tuscaloosa, AL, pp 1–12

Edwards SV, Robin VV, Ferrand N, Moritz C (2022) The evolution of comparative phylogeography: putting the geography (and more) into comparative population genomics. Genome Biol Evolut 4:14

Environmental Protection Agency, 2024, epa.gov. "Level III and IV Ecoregions by State", accessed 16 July 2024 https://www.epa.gov/eco-research/ecoregion-download-files-state-region-6#pane-34

Ersts PJ (2023) Geographic distance matrix generator (version 1.2.3). American Museum of Natural History, Center for Biodiversity and Conservation. Available from http://biodiversityinformatics.amnh.org/open_source/gdmg. Accessed on 2023–8–7.

Excoffier L, Smouse PE, Quattro JM (1992) Analysis of molecular variance inferred from metric distances among DNA haplotypes – application to human mitochondrial-DNA restriction data. Genetics 131:479–491

Excoffier L, Laval G, Schneider S (2005) Arlequin (version 3.0): an integrated software package for population genetics data analysis. Evol Bioinform Online 1:47–50

Fischer MC, Foll M, Excoffier L, Heckel G (2011) Enhanced AFLP genome scans detect local adaptation in high-altitude populations of a small rodent (Microtus arvalis). Mol Ecol 20:1450–1462

Foll M, Gaggiotti OE (2008) A genome scan method to identify selected loci appropriate for both dominant and codominant markers: a bayesian perspective. Genetics 180:977–993

Folmer O, Black M, Hoeh W, Lutz R, Vrijenhoek R (1994) DNA primers for amplification of mitochondrial cytochrome c oxidase subunit I from diverse metazoan invertebrates. Mol Mar Biol Biotech 3:294–299

Freeland JR (2020) Molecular ecology, 3rd edn. John Wiley and Sons, Hoboken, NJ

Frichot E, François O (2015) LEA: An R package for landscape and ecological association studies. Methods Ecol Evol 6:925–929

Gang C, Zhou W, Che Y, Wang Z, Sun Z, Li J, Qi J, Odeh I (2014) Quantitative assessment of the contributions of climate change

and human activities on global grassland degradation. Environmental Earth Sci 72:4273–4282
Ghisbain G, Lozier JD, Rahman SR, Ezray BD, Tian L, Ulmer JM, Heraghty SD, Strange JP, Rasmont P, Hines HM (2020) Substantial genetic divergence and lack of recent gene flow support cryptic speciation in a colour polymorphic bumble bee (*Bombus bifarius*) species complex. Syst Entomol 45:635–652
Goudet J, Jombart T (2022) _hierfstat: Estimation and tests of hierarchical F-statistics. R package version 0.5–11.
Grainger TN, Germain RM, Jones NT, Gilbert B (2017) Predators modify biogeographic constraints on species distributions in an insect metacommunity. Ecology 98:851–860
Gutenkunst RN, Hernandez RD, Williamson SH, Bustamante CD (2009) Inferring the joint demographic history of multiple populations from multidimensional SNP frequency data. PLoS Genet 5:e1000695
Gutiérrez-Trejo N, Van Dam MH, Lam AW et al (2024) Phylogenomics of *Tetraopes* longhorn beetles unravels their evolutionary history and biogeographic origins. Sci Rep 14:7285
Hebert PDN, Ratnasingham S, deWaard JR (2003) Barcoding animal life: cytochrome oxidase subunit 1 divergences among closely related species. Proc Royal Soc B-Biol Sci 270:S96–S99
Hill JG (2015) Revision and biogeography of the *Melanopus Scudderi* species group (*Orthoptera*: *Acrididae*: *Melanopinae*) with a description of 21 new species and establishment of the carnegiei and davisi species groups. Trans Am Entomol Soc 141(2):252–350
Hill JG, Barone JA (eds) (2018) Southeastern grasslands: biodiversity, ecology, and management, 1st edn. The University of Alabama Press, Tuscaloosa, AL
Jombart T, Ahmed I (2011) adegenet 1.3-1: new tools for the analysis of genome-wide SNP data. Bioinformatics 27:3070–3071
Jouganous J, Long W, Ragsdale AP, Gravel S (2017) Inferring the joint demographic history of multiple populations: beyond the diffusion approximation. Genetics 206:1549–1567
Kawamura K, Parrenin F, Lisiecki L, Uemura R, Vimeux F, Severinghaus JP, Hutterli MA, Nakazawa T, Aoki S, Jouzel J, Raymo ME, Matsumoto K, Nakata H, Motoyama H, Fujita S, Goto-Azuma K, Fujii Y, Watanabe O (2007) Northern hemisphere forcing of climatic cycles in Antarctica over the past 360,000 years. Nature 448:912-U914
Keightley PD, Pinharanda A, Ness RW, Simpson F, Dasmahapatra KK, Mallet J, Davey JW, Jiggins CD (2015) Estimation of the spontaneous mutation rate in *Heliconius melpomene*. Mol Biol Evol 32:239–243
Knaus BJ, Grünwald NJ (2017) VCFR: a package to manipulate and visualize variant call format data in R. Mol Ecol Resour 17:44–53
Kress WJ, Garcia-Robledo C, Uriarte M, Erickson DL (2015) DNA barcodes for ecology, evolution, and conservation. Trends Ecol Evol 30:25–35
Laikre L, Allendorf FW, Aroner LC, Baker CS, Gregovich DP, Hansen MM, Jackson JA, Kendall KC, McKelvey K, Neel MC, Olivieri I, Ryman N, Schwartz MK, Bull RS, Stetz JB, Tallmon DA, Taylor BL, Vojta CD, Waller DM, Waples RS (2010) Neglect of genetic diversity in implementation of the convention on biological diversity. Conserv Biol 24:86–88
Lawrence WS (1988) Movement ecology of the Red Milkweed Beetle in relation to population size and structure. J Animal Ecol 57:21
Leigh JW, Bryant D (2015) POPART: full-feature software for haplotype network construction. Methods Ecol Evol 6:1110–1116
Lingafelter SW (2007) Illustrated key to the longhorned woodboring beetles of the eastern United States. Special Publication No. 3. Coleopterists Society Miscellaneous Publication.
Linsley GE (1995) The cerambycidae of North America, Part VII tribe tetraopini. Univ California Publicat Entomol 2:250–279
Liu HX, Jia YX, Sun XG, Tian DC, Hurst LD, Yang SH (2017) Direct determination of the mutation rate in the bumblebee reveals evidence for weak recombination-associated mutation and an approximate rate constancy in insects. Mol Biol Evol 34:119–130
MacRae TC (1993) Annotated checklist of the longhorned beetles (*Coleoptera*: *Cerambycidae* and *Disteniidae*) occurring in missouri. Insecta Mundi 7:4
MacRoberts MH, MacRoberts BR, Jackson LS (2003) Louisiana prairies. In: Peacock E, Schauwecker T (eds) Blackland prairies of the Gulf Coastal Plain, 1st edn. The University of Alabama Press, Tuscaloosa, AL, pp 80–93
Noskova E, Borovitskiy V (2023) Bayesian optimization for demographic inference. G3-Genes Genomes Genetics. https://doi.org/10.1093/g3journal/jkad080
Noss RF (2013) Forgotten grasslands of the south: Natural history and conservation, 1st edn. Island Press, Washington DC
Oksanen J, Simpson G, Blanchet F, Kindt R, Legendre P, Minchin P, O'Hara R, Solymos P, Stevens M, Szoecs E, Wagner H, Barbour M, Bedward M, Bolker B, Borcard D, Carvalho G, Chirico M, De Caceres M, Durand S, Evangelista H, FitzJohn R, Friendly M, Furneaux B, Hannigan G, Hill M, Lahti L, McGlinn D, Ouellette M, Ribeiro Cunha E, Smith T, Stier A, Ter Braak C, Weedon J (2022) _vegan: Community ecology package_. R package version 2.6–4.
Oppold AM, Pfenninger M (2017) Direct estimation of the spontaneous mutation rate by short-term mutation accumulation lines in *Chironomus riparius*. Evolution Letters 1:86–92
Peacock E, Schauwecker T (2003) Blackland prairies of the gulf coastal plain, 1st edn. The University of Alabama Press, Tuscaloosa, AL
Phillipsen IC, Kirk EH, Bogan MT, Mims MC, Olden JD, Lytle DA (2015) Dispersal ability and habitat requirements determine landscape-level genetic patterns in desert aquatic insects. Mol Ecol 24:54–69
Rice ME (1988) Natural history observations on *Tetraopes* and other *Cerambycidae* (*Coleoptera*) from the great plains ecosystem. J Kansas Entomol Soc 61:4
Rochette NC, Rivera-Colon AG, Catchen JM (2019) Stacks 2: analytical methods for paired-end sequencing improve RADseq-based population genomics. Mol Ecol 28:4737–4754
Scheifer TL (1998) Disjunct distribution of cerambycidae (*Coleoptera*) in the black belt prairie and jackson prairie in mississippi and alabama. Coleopt Bull 52(3):278–284
Schotz A, Barbour M (2009) Ecological assessment and terrestrial vertebrate surveys for Black Belt Prairies in Alabama. Submitted to Alabama Department of Conservation and Natural Resources, Division of Wildlife & freshwater Fisheries.
Smouse PE, Long JC, Sokal RR (1986) Multiple regression and correlation extensions of the mantel test of matrix correspondence. Syst Zool 35:627–632
Stobie CS, Cunningham MJ, Oosthuizen CJ, Bloomer P (2019) Finding stories in noise: mitochondrial portraits from RAD data. Mol Ecol Resour 19:191–205
Toro MA, Caballero A (2005) Characterization and conservation of genetic diversity in subdivided populations. Philosophical Trans Royal Soc B-Biol Sci 360:1367–1378
USDA, NRCS. 2024. The PLANTS Database (http://plants.usda.gov, 04/10/2024). National Plant Data Team, Greensboro, NC USA.
Vidal MC, Quinn TW, Stireman JO, Tinghitella RM, Murphy SM (2019) Geography is more important than host plant use for the population genetic structure of a generalist insect herbivore. Mol Ecol 28:4317–4334
Warriner MD (2004) Scientific note: occurrence and conservation status of the milkweed beetle *Tetraopes texanus* Horn (*Coleoptera*: *Cerambycidae*) in Arkansas. Coleopt Bull 58:4

Weir BS, Cockerham CC (1984) Estimating F-statistics for the analysis of population structure. Evolution 38:1358–1370
Whiles M, Charlton RE (2006) The ecological significance of tallgrass prairie arthropods. Annu Rev Entomol 51:387–412
Wilsey BJ (2018) The biology of grasslands, 1st edn. Oxford University Press, Oxford, UK
Wright EK (1987) Stratification and paleocirculation of the late cretaceous wester interior seaway of North America. Geol Soc Am Bull 99:480–490
Xue AT, Hickerson MJ (2020) Comparative phylogeographic inference with genome-wide data from aggregated population pairs. Evolution 74:808–830
Zayed A, Packer L, Grixti JC, Ruz L, Owen RE, Toro H (2005) Increased genetic differentiation in a specialist versus a generalist bee: implications for conservation. Conserv Genet 6:1017–1026